

# Conformation specific and charge directed reactivity of radical cation intermediates of $\alpha$ -substituted (amino, hydroxy, and keto) bioactive carboxylic acids†

Atanu Bhattacharya,‡ Joong-Won Shin, Keven J. Clawson and Elliot R. Bernstein\*

Received 23rd February 2010, Accepted 26th April 2010

DOI: 10.1039/c003416a

The reactivity of radical cation carboxylic acids is investigated on the basis of mass spectrometry, infrared-vacuum ultraviolet (IR-VUV) photoionization spectroscopy, and high level correlated *ab initio* calculations. Their reactivity is found to be highly conformation specific and is governed by their initial charge distribution following ionization. In the present work, the radical cations of lactic acid, pyruvic acid, glycine, and valine are studied to probe their stability and conformation specific reactivity following single photon, vertical ionization at 10.5 eV. For lactic acid, glycine, and valine, the localization site of the hole following sudden removal of an electron depends on their specific intramolecular hydrogen bonding network. Lactic acid, glycine, and valine undergo complete fragmentation following vertical ionization at 10.5 eV; however, pyruvic acid does not completely dissociate following vertical ionization. Only 45% of the pyruvic acid parent ions undergo  $C_{\alpha}$ - $C_{\text{carboxylic}}$  bond dissociation. If the hole is localized on the COOH moiety of glycine, valine, and lactic acid, a hydrogen transfer is favored from the COOH to the  $\alpha$ -substituent. If the hole is localized on the  $\alpha$ -hydroxy or -amine substituent and the singly occupied molecular orbital (SOMO, where the hole resides) is parallel to the  $C_{\alpha}$ - $C_{\text{carboxylic}}$  bond,  $C_{\alpha}$ - $C_{\text{carboxylic}}$  bond dissociation occurs through charge transfer from the  $\alpha$ -substituent to the  $C_{\alpha}$ - $C_{\text{carboxylic}}$  bond. The present study reveals that the specific conformations of  $\alpha$ -substituted carboxylic acids govern their radical cationic reactivity. The radical cation of pyruvic acid exhibits a special stability due to enolization of the  $\alpha$ -keto form on the cationic surface.

## Introduction

Radical cation intermediates of  $\alpha$ -substituted carboxylic acid based biological building blocks, such as amino acids, peptides and proteins, lactic acid, and pyruvic acid, have major roles in biochemistry and medicinal chemistry,<sup>1</sup> and are responsible for the development of a wide range of human physiological disorders.<sup>2,3</sup> In the past few years, the properties of different bioactive carboxylic acid derived radicals have attracted considerable attention, both from experimental<sup>4–10</sup> and theoretical points of view.<sup>11–22</sup>

The location of the charge and hydrogen bonding in a radical cation is of great importance for its reactivity and stability.<sup>23</sup> One of the most important aspects of the reaction dynamics of radical cation intermediates of peptides involves an extremely rapid (subfemtosecond) transfer of charge<sup>24</sup> and alteration of their reactivity due to variation of local sites for ionization.<sup>23</sup> Recent theoretical studies have predicted that charge migration in radical cations of glycine, following the removal of an electron from three different orbitals, strongly

depends on specific orientations of the atoms in the molecule (conformations).<sup>25</sup> Such charge migration can lead to distinct reaction dynamics for different glycine conformers;<sup>26</sup> however, this prediction has not yet been experimentally confirmed.

The flexibility of three dimensional structures of  $\alpha$ -substituted bioactive carboxylic acids permits great conformational diversity. Different conformers can interconvert *via* hindered rotations about single bonds, giving rise to conformational isomerism. The behavior of these ionized conformers can be governed by their initial detailed molecular structures. Therefore, a detailed characterization of conformation specific reactivity of radical cation intermediates of  $\alpha$ -substituted bioactive carboxylic acids would be invaluable for understanding the phenomenon of oxidative stress at a molecular level. A few studies of conformer selective dynamics of isolated radical cation intermediates of  $\alpha$ -substituted bioactive carboxylic acids have recently appeared in literature.<sup>26,27</sup>

For unambiguous tracking of a conformation specific biochemical reaction and its dynamics, isolation, identification, and fragmentation behavior of conformations are essential prerequisites. We carry out such an analysis using a supersonic jet expansion to obtain an internal temperature low enough to suppress interconversion between different conformers of lactic acid ( $\alpha$ -hydroxy acid), pyruvic acid ( $\alpha$ -keto acid), and glycine and valine ( $\alpha$ -amino acids). Once the conformers are trapped in different local minima of their ground state potential

Department of Chemistry, Colorado State University, Fort Collins, CO 80523-1872, USA. E-mail: erb@lamar.colostate.edu

† Electronic supplementary information (ESI) available: Theoretical details. See DOI: 10.1039/c003416a

‡ Current address: Chemistry Department, Brookhaven National Laboratory, Upton, NY 11973-5000, USA.

energy surfaces (PESs), conformation specific fragmentation patterns for radical cation intermediates are proven by observing different infrared (IR) spectra (corresponding to different conformers) obtained at different mass spectrometric fragment signals generated through the ionization process. The experimental studies are accompanied by highly correlated *ab initio* calculations at the MP2 and CASSCF levels of theory. The conformation specific differences in reactivity are explained by conformation mediated localization of the positive charge (or hole) on the radical cations formed through single photon vacuum ultraviolet (10.5 eV) ionization.

## Experimental methods

The experimental setup used to record time of flight mass spectra and IR-VUV ionization spectra has been previously described in detail.<sup>28</sup> Lactic acid and pyruvic acid are placed behind a pulsed valve body (Parker General Valve series 9) and are heated to about 50 °C to increase their vapor pressure. The gaseous molecules are brought into the molecular beam by a neon/helium gas mixture (69%/31%) at 30 psig backing pressure. After passing through a skimmer, the molecular beam interacts with pulsed VUV and IR laser beams in the ionization region of a time of flight mass spectrometer.

The IR laser beam, which precedes by 70 ns and counter-propagates with respect to the 118 nm laser beam, is focused at the VUV/molecular beam interaction point by a 80 cm focal length lens to probe neutral ground state species. The 118 nm radiation is the ninth harmonic of the fundamental output of a Nd:YAG laser at 1064 nm. 355 nm radiation (third harmonic) of the Nd:YAG laser is focused into a cell filled with Xe/Ar at a ratio of 1:10 at 200 Torr total pressure. An MgF<sub>2</sub> lens focuses the 118 nm light in the ionization region of the time of flight mass spectrometer (TOFMS) and disperses the remaining 355 nm light. The tunable IR laser output generated by an OPO/OPA system (LaserVision), pumped by 532 nm radiation from another Nd:YAG laser, has an energy of 3-5 mJ/pulse and a bandwidth of ~2 cm<sup>-1</sup> in the 2800–3800 cm<sup>-1</sup> range.

## Theoretical methods

For rigorous descriptions of the PES of radical cationic bio-active carboxylic acids, highly correlated multiconfigurational methods are necessary.<sup>29</sup> These multiconfigurational methodologies are particularly important for calculating surfaces with “near degeneracy effects” caused by presence of conical intersections between the many low lying valence ion states. Ground electronic surface topology is often found<sup>29</sup> to be altered by proximity of an upper excited electronic state surface along a particular reaction coordinate near a conical intersection, which can only be calculated through multiconfigurational methods. Monoconfigurational methods such as HF or MP2 often overestimate or underestimate the energy barrier to a transition state on the ground electronic surface of the radical ion near conical intersections. Illustrations of such a consideration are found recently for many organic compounds.<sup>30</sup> Therefore, in the present work, exploration of cationic PESs is performed using the CASSCF level of theory. Furthermore, a number of configurations are expected to

contribute to a particular electronic state of the radical cations. In fact, for glycine the  $n\sigma_{\text{O}}$  and  $n\pi_{\text{O}}$  configurations have equal weight (0.5) near the  $(D_1/D_0)_{\text{CI}}$  on the ground cationic PES. The use of multiconfigurational methodology to explore PESs of the radical cationic lactic acid, glycine, valine, and pyruvic acid is thereby mandatory. In order to calculate dynamic correlation, more expensive CASMP2 or CCSD(T) can be used; however, dynamical correlation energy is not always a contributing factor to the total energy. In particular, CASMP2 results do not improve the energetics significantly for the radical cation intermediates studied here. Thus the less expensive CASSCF level of theory with a 6-31G(d) basis set is used in the present study. Improving the basis set does not significantly improve the energetics at the CASSCF level of theory as long as a balanced active space is employed.<sup>31</sup>

All geometry optimizations relevant to the ion state decomposition of lactic acid, pyruvic acid, glycine, and valine are carried out at the CASSCF/6-31G(d) and MP2/aug-cc-pVDZ levels of theory using the Gaussian 03<sup>32</sup> and MOLPRO<sup>33</sup> programs. To explore the ion state PESs, the active space comprises 9 electrons distributed in 8 orbitals, denoted as CASSCF(9,8). The orbitals used in the active space of lactic acid, pyruvic acid, glycine, and valine are illustrated in Figure S1 in the Supporting Information. We determine the lowest vertical ionization energy ( $E_{\text{VI}}$ ) by explicitly calculating the energy difference between the neutral and cation at the Franck–Condon geometry employing the MP2/aug-cc-pVDZ level of theory. Critical points (minima and transition states) are characterized by analytical frequency calculations. Minimum energy paths are calculated using an intrinsic reaction coordinate (IRC) algorithm implemented in the Gaussian 03 program suite. Conical intersection searches are performed using the algorithm implemented in Gaussian 03.

## Experimental results

### Lactic acid

Lactic acid has three internal rotation axes that can give rise to a number of conformational isomers. It also has a chiral carbon which leads to the existence of enantiomers. As IR-VUV photoionization spectroscopy is not sensitive to molecular chirality effects, identification of different enantiomers of lactic acid is not possible using this spectroscopic technique; however, this technique can identify different conformers of lactic acid present in the molecular beam.

The three lowest energy conformers of neutral lactic acid with calculated (MP2/aug-cc-pVDZ) relative energies (in kcal/mol) are depicted in Fig. 1. These results are in agreement with previous theoretical calculations,<sup>34</sup> and the available microwave<sup>35</sup> and FTIR<sup>36</sup> spectroscopy data. The conformers differ mainly by different types of intramolecular hydrogen bonding linkages: O–H $\cdots$ O=C (conformer I), O–H $\cdots$ O(H)CO (conformer II), and C(O)O–H $\cdots$ O–H (conformer III). Conformer I in Fig. 1 represents the lowest energy conformer. The remaining possible conformers, which are not shown in the figure, are estimated to have a total population of less than 0.1% at 298 K,<sup>36</sup> and therefore is disregarded in the present study.

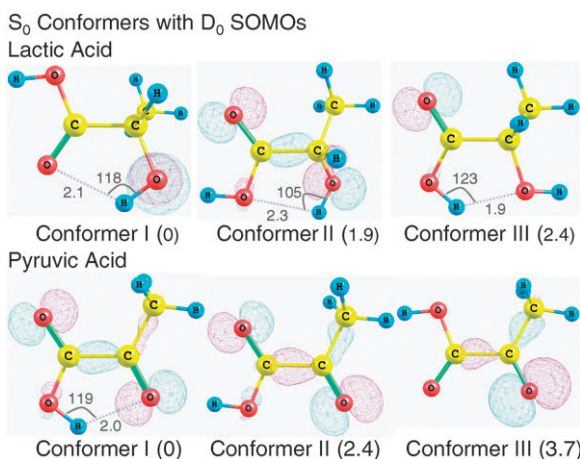


**Fig. 1** The three lowest energy conformers of ground state ( $S_0$ ) neutral lactic acid and pyruvic acid with calculated (MP2/aug-cc-pVDZ) relative energies (in kcal/mol), showing their bond distances and bond angles. The density plots for the SOMO (singly occupied molecular orbital) of lactic acid and pyruvic acid at the Franck–Condon point on the cationic  $D_0$  surface calculated at the CASSCF(9,8)/6-31G(d) level of theory are also shown. The two colors for these orbitals indicate the plus and minus phases of the wavefunctions.

Fig. 2 shows the TOF mass spectrum of lactic acid obtained through single photon ionization at 10.5 eV. The ion signals at  $m/z = 44$  and 30 amu correspond to  $H_3CC(H)CO^+$  and  $HCOH^+$  fragments, respectively. The absence of a parent ion signal indicates that lactic acid undergoes complete molecular fragmentation following single photon vertical ionization at 10.5 eV. The more intense fragment ion signal at  $m/z = 44$  amu in the mass spectrum can be assigned to a product resulting from the intramolecular hydrogen transfer from the  $\alpha$ -OH to the COOH group followed by the breaking of the  $C_{\alpha}-C_{\text{carboxylic}}$  bond from either conformer I or II. This fragment ion signal cannot be generated from conformer III because the hydrogen bond is formed by the carboxylic acid OH group's H atom bonding to the  $\alpha$ -OH group. The ion signal at  $m/z = 30$  amu can be attributed to a product formed upon direct  $C_{\alpha}-C_{\text{carboxylic}}$  bond dissociation followed by the elimination of the  $CH_3$  radical from all three lowest energy conformers of lactic acid. Therefore, with the diversity of different possible fragmentation pathways for each conformer, the TOFMS alone does not enable us to identify unambiguously the fragmentation patterns of the radial cation intermediates of lactic acid in a conformation specific way. IR-VUV photoionization spectroscopy can, however, aid in such analysis.

The infrared spectra of lactic acid, recorded by monitoring the fragment signals at  $m/z = 44$  and 30 amu obtained through IR-VUV spectroscopy, are presented in Fig. 3. Enhancement of the ion signal intensity is observed at both fragment mass channels when the IR radiation is absorbed by a characteristic normal mode of vibration for a specific conformer of lactic acid. Several calculated (MP2/aug-cc-pVDZ) scaled (0.96) harmonic vibrational frequencies are also displayed in Fig. 3 below the experimental spectra, with their corresponding conformers. The IR spectra obtained at fragment mass channels of  $m/z = 44$  and 30 amu are in good agreement with the scaled

Lactic Acid 10.5 eV Ionization

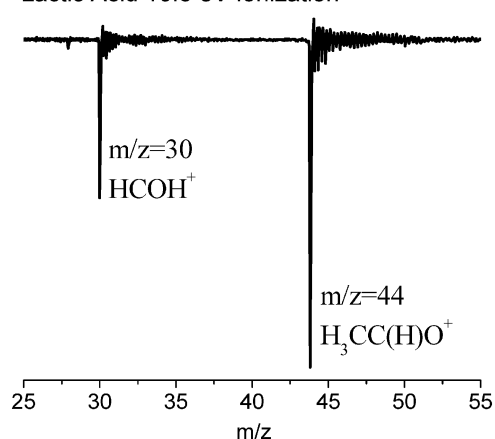


**Fig. 2** Time of flight mass spectrum for lactic acid ionized at 10.5 eV.

(0.96) harmonic calculated IR frequencies of conformers I and II, respectively.

A qualitative assignment of the IR spectra can be generated by considering the OH vibrational mode energy in light of its involvement with hydrogen bonding. Hydrogen bonding in the molecular system is responsible for the red shift ( $100\text{--}300\text{ cm}^{-1}$  depending on the strength of H-bond) in the  $\nu_{OH}$  stretch vibrational frequency compared to the free (non hydrogen bonded) OH stretching mode.<sup>37</sup> Additionally, absorption of an OH stretching mode associated with a hydrogen bonded OH moiety is also often broadened due to complex anharmonic coupling mechanisms involving normal modes associated with the O–H...O hydrogen bond forming atoms and other overtone and combination modes.<sup>38</sup>

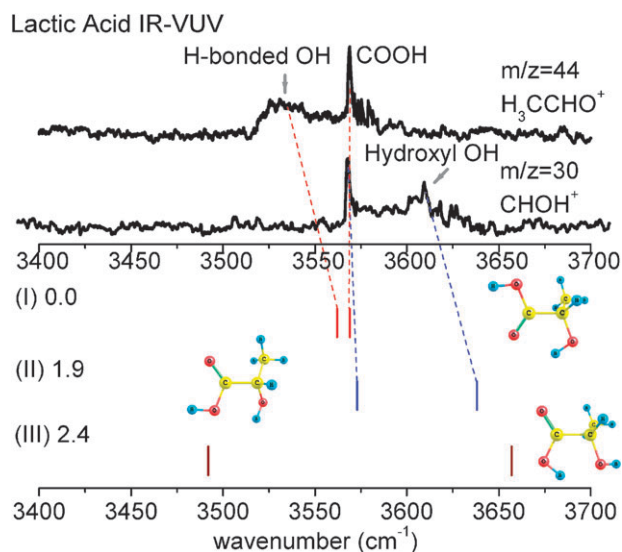


**Fig. 3** IR-VUV spectra of lactic acid recorded monitoring fragment signals at  $m/z = 44$  and 30 amu in the region of free or hydrogen bonded OH stretching modes. Colored vertical bars represents calculated (MP2/aug-cc-pVDZ), scaled (0.96), harmonic frequencies for the different conformers of lactic acid. For conformer I, the left vertical bar indicates the hydrogen bonded OH stretch. For conformer II, the right vertical bar indicates hydrogen bonded OH stretch.

The above considerations are clearly pertinent for the spectra in Fig. 3. Sharp peaks corresponding to the free carboxylic acid OH stretch (near  $3569\text{ cm}^{-1}$ ) are observed in both spectra. A broad feature appears to the red of the free carboxylic acid OH stretch in the IR spectrum obtained at fragment mass channel  $m/z = 44$  amu; this feature can be assigned as a relatively strongly hydrogen bonded hydroxyl OH stretch. A sharp feature appears to the blue of the free carboxylic acid OH stretch in the IR spectrum recorded at fragment mass channel  $m/z = 30$  amu; this feature can be attributed to a relatively free non hydrogen bonded hydroxyl OH stretch. The relative positions of the hydroxyl OH stretching mode (either hydrogen bonded or free) in the two spectra provide qualitative information about the relative strength of O–H...O intramolecular interaction for conformers I and II. The larger red shift of the hydroxyl OH oscillator of conformer I confirms that this conformer possesses a stronger O–H...O hydrogen bond interaction. Absence of a strongly red shifted hydroxyl OH oscillator in conformer II corroborates a weak interaction between the  $\alpha$ -hydroxy OH and COOH groups. The mismatch between experimental and theoretical results for hydrogen bonded or free hydroxyl OH frequencies in the spectra presumably arises due to strong anharmonic coupling and coupling between the harmonic frequency mode and low frequency combination modes, which are not considered in the calculation at the MP2/aug-cc-pVDZ level of theory. The qualitative observation of a red shift of more than  $130\text{ cm}^{-1}$  associated with the hydrogen bonding effect for conformer I is, however, well reproduced in the calculation. Therefore, the relative positions of hydroxyl OH stretching mode (either hydrogen bonded or free) in the two spectra provide clear information about the relative strength of O–H...O intramolecular interaction for conformers I and II.

Furthermore, since a free hydroxyl OH vibration is observed at  $3610\text{ cm}^{-1}$  by monitoring the fragment signal at  $m/z = 30$  amu, one can conclude that conformer I has no significant contribution to the ion signal at  $m/z = 30$  amu. No hydrogen bonded carboxylic acid OH stretch frequency is observed in either of these spectra; thus the conformer III does not contribute to either the fragment signal at  $m/z = 44$  or  $30$  amu.

### Pyruvic acid

Fig. 1 depicts the three lowest energy conformers of neutral pyruvic acid with their calculated (MP2/aug-cc-pVDZ) relative energies (in kcal/mol). The conformers differ by the type of hydrogen bonding, and relative orientation of the  $\alpha$ -keto group with respect to the COOH group. Conformer I is the lowest energy conformer, which is in agreement with the literature.<sup>39,40</sup> The TOF mass spectrum of pyruvic acid obtained using single photon ionization at  $10.5\text{ eV}$  is depicted in Fig. 4. The spectrum contains a parent ion signal at  $m/z = 88$  amu and one fragment signal, corresponding to  $\text{H}_3\text{CCO}^+$ , at  $m/z = 43$  amu. The fragment ion signal at  $m/z = 43$  amu can be attributed to a product resulting from direct  $\text{C}_\alpha\text{--C}_{\text{carboxylic}}$  bond dissociation from all three low energy conformers. Further identification of the different conformers contributing to the direct  $\text{C}_\alpha\text{--C}_{\text{carboxylic}}$  bond

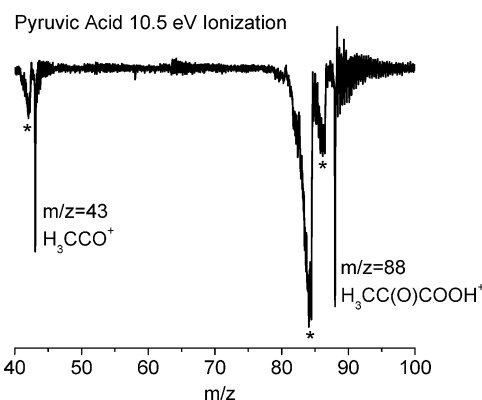


**Fig. 4** Time of flight mass spectrum for pyruvic acid ionized at  $10.5\text{ eV}$ . The ion signals denoted by \* are due to diffusion pump oil which was present in the vacuum chamber.

dissociation channel is performed using IR-VUV photoionization spectroscopy.

The infrared spectrum, obtained by monitoring the pyruvic acid parent ion signal at  $m/z = 88$  amu, is given in Fig. 5. No vibrational features are observed in the  $m/z = 43$  amu mass channel. An enhancement in ion signal intensity is observed at the mass channel  $m/z = 88$  amu (parent ion signal) when IR radiation is absorbed by a specific normal mode of vibration for a particular conformer of pyruvic acid. Enhancement of the parent ion signal intensity in the presence of IR radiation arises due to the enhancement in ionization cross section of the parent molecule from its vibrationally excited states. The IR spectrum in Fig. 5 displays two features resulting from the two different environments of the carboxylic acid OH bond: one is associated with the free OH stretch ( $3582\text{ cm}^{-1}$ ) and other is associated with the hydrogen bonded carboxylic acid OH stretch ( $3460\text{ cm}^{-1}$ ). The sharp feature in the spectrum at  $3582\text{ cm}^{-1}$  exhibits an excellent fit with the calculated IR frequency of the free carboxylic acid OH stretch for conformers II and III, which is also in good agreement with recent FTIR measurements.<sup>40</sup> The broad feature to the red of the free OH stretch in the spectrum can be ascribed to a hydrogen bonded carboxylic OH stretch, which is qualitatively consistent with the calculated vibrational frequency of hydrogen bonded carboxylic acid OH stretch for conformer I. The free carboxylic acid OH stretch observed at  $3582\text{ cm}^{-1}$  is also in agreement with the calculated vibrational frequency for the conformer III; however, this conformer is estimated to have total population less than 0.2% at 300 K using a Boltzmann population distribution, and therefore, has been considered to contribute little to the present study. We can, thus, conclude that both conformers I and II are present in the molecular beam. The only fragment signal observed following single photon ionization of pyruvic acid at  $10.5\text{ eV}$  corresponds to  $\text{H}_3\text{CCO}^+$ , at  $m/z = 43$  amu; in principle, it can be generated from both of these two conformers. The fragmentation mechanism will be further explored using theoretical calculations.

### Glycine and valine

To probe conformation specificity for the reactivity of radical cationic glycine and valine we reillustrate here the results for

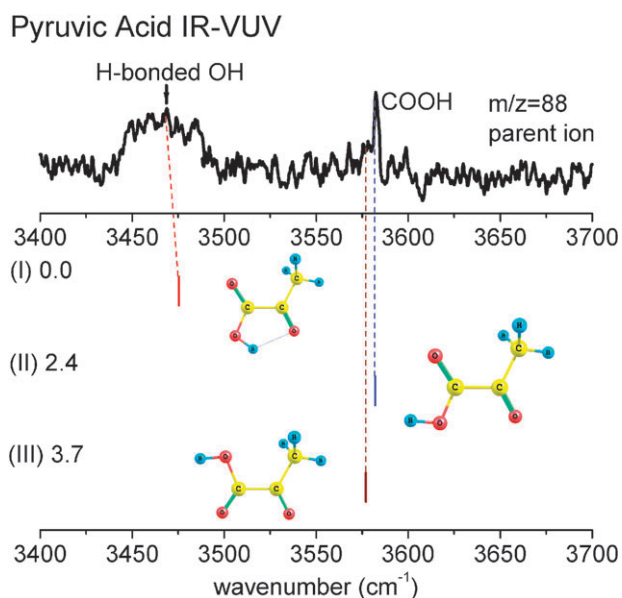


**Fig. 5** IR-VUV spectra of pyruvic acid recorded monitoring the parent ion signal at  $m/z = 88$  amu in the region of free or hydrogen bonded OH stretching modes. Colored vertical bars represent calculated (MP2/aug-cc-pVDZ), scaled (0.96), harmonic frequencies for the different conformers of pyruvic acid.

these two molecules that were previously experimentally examined by our group.<sup>41</sup> We here reexamine some of those results in order to assess conformation specificity for the reactivity of radical cationic glycine and valine.

Three lowest energy conformers of neutral glycine and valine, which differ again mainly by different types of intramolecular hydrogen bonding linkages, are illustrated in Fig. 6. Single photon ionization of glycine at 10.5 eV reveals two intense fragment signals at  $m/z = 30$  and 31 amu along with weaker fragment signals at  $m/z = 42$  and 43 amu.<sup>41</sup> The fragment signal at  $m/z = 30$  amu ( $\text{H}_2\text{CNH}_2^+$ ) can be attributed to a product formed upon direct  $\text{C}_\alpha\text{-C}_{\text{carboxylic}}$  bond dissociation from all three conformers of glycine. The fragment signal at  $m/z = 31$  amu ( $\text{H}_2\text{CNH}_3^+$ ) can be assigned to a product formed upon hydrogen transfer from the COOH to the  $\alpha\text{-NH}_2$  group followed by  $\text{C}_\alpha\text{-C}_{\text{carboxylic}}$  bond dissociation. No IR spectrum could be recorded monitoring the fragment signal at  $m/z = 31$  amu; however, in our original previous study,<sup>41</sup> an IR spectrum is obtained monitoring the fragment signal at  $m/z = 30$  amu, which is reproduced in Fig. 7. The IR spectrum reveals three distinct features that arise due to free symmetric ( $3360\text{ cm}^{-1}$ ) and asymmetric ( $3440\text{ cm}^{-1}$ )  $\text{NH}_2$  stretches and a free carboxylic acid OH stretch ( $3587\text{ cm}^{-1}$ ). This assignment is consistent with the calculated scaled harmonic vibrational frequencies for conformers I and III of glycine. No hydrogen bonded carboxylic acid OH stretch is observed in the IR spectrum obtained at the ion signal of  $m/z = 30$  amu, which indicates that the fragment  $\text{H}_2\text{CNH}_2^+$  is not generated from conformer II through  $\text{C}_\alpha\text{-C}_{\text{carboxylic}}$  bond dissociation. Only conformers I and III, instead, follow the  $\text{C}_\alpha\text{-C}_{\text{carboxylic}}$  bond dissociation pathway.

The fragment signal at  $m/z = 31$  amu ( $\text{H}_2\text{CNH}_3^+$ ) is unique with regard to the possible fragmentation mechanism

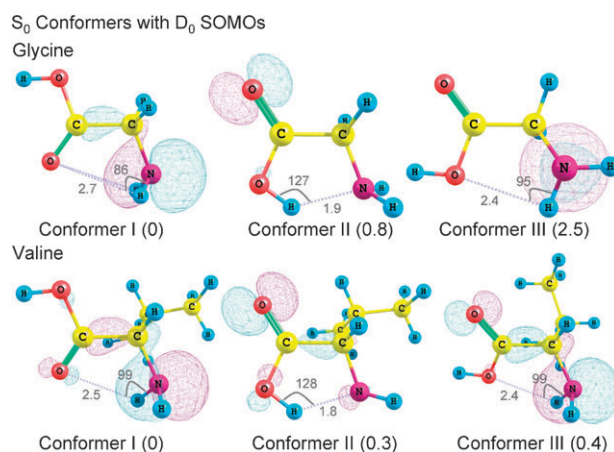


**Fig. 6** The three lowest energy conformers of ground state ( $S_0$ ) neutral glycine and valine with calculated (MP2/aug-cc-pVDZ) relative energies (in kcal/mol), showing their bond distances and bond angles. The density plots for the SOMO (singly occupied molecular orbital) of glycine and valine at the Franck–Condon point on the cationic  $D_0$  surface calculated at the CASSCF(9,8)/6-31G(d) level of theory are also shown. The two colors for these orbitals indicate the plus and minus phases of the wavefunctions.

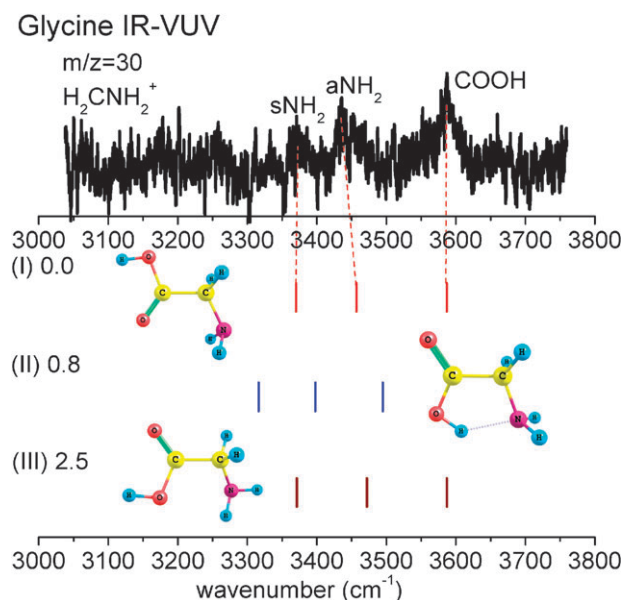


**Fig. 7** IR-VUV spectra of glycine recorded monitoring the fragment ion signal at  $m/z = 30$  amu in the region of free or hydrogen bonded OH stretching mode and  $\text{NH}_2$  stretching mode. Colored vertical bars represent calculated (MP2/aug-cc-pVDZ), scaled (0.96), harmonic frequencies for the different conformers of glycine. The IR spectrum is reproduced from ref. 41.

of the glycine radical cation because it can only be generated from conformer II through a hydrogen transfer from the COOH group to the  $\alpha\text{-NH}_2$  group followed by  $\text{C}_\alpha\text{-C}_{\text{carboxylic}}$  bond dissociation. Thus, one can conclude that the fragment  $\text{CH}_2\text{NH}_3^+$  results from conformer II: this assignment is experimentally demonstrated<sup>41</sup> using an equivalent fragment signal of valine obtained at  $m/z = 73$  amu ( $(\text{CH}_3)_2\text{C}(\text{H})\text{C}(\text{H})\text{NH}_3^+$ ).

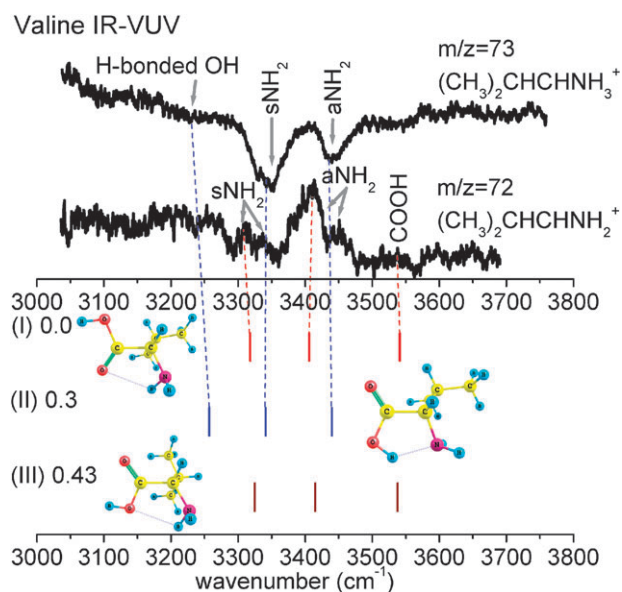


**Fig. 8** IR-VUV spectra of valine recorded monitoring the fragment signal at  $m/z = 72$  and  $73$  amu in the region of OH and  $\text{NH}_2$  stretching modes. Colored vertical bars represent calculated (MP2/aug-cc-pVDZ), scaled (0.96), harmonic frequencies for different conformers of valine. The IR spectra are reproduced from ref. 41.

Single photon ionization of valine at 10.5 eV exhibits fragment signals at  $m/z = 30$ , 72, and 73 amu.<sup>41</sup> The fragment signal at  $m/z = 73$  amu can be related to a product formed upon a hydrogen transfer from COOH to the  $\alpha$ - $\text{NH}_2$  group followed by  $\text{C}_\alpha$ - $\text{C}_{\text{carboxylic}}$  bond dissociation. The IR spectrum (Fig. 8) obtained at this fragment mass channel (negative) reveals a broad feature below  $3300\text{ cm}^{-1}$ , corresponding to a hydrogen bonded carboxylic acid OH, and two distinguishable bands, which arise from free symmetric ( $3346\text{ cm}^{-1}$ ) and asymmetric ( $3436\text{ cm}^{-1}$ )  $\text{NH}_2$  stretches. This assignment is also in agreement with the calculated scaled harmonic vibrational frequencies for conformer II of valine. The noticeable broadening of each feature associated with symmetric and asymmetric  $\text{NH}_2$  stretching modes in the spectrum possibly arises from almost free rotation of the isopropyl group along the  $\text{C}_\alpha$ - $\text{C}_\beta$  bond in valine, which renders two additional conformers each retaining the hydrogen bonded network in the  $\alpha$ -amino carboxylic acid moiety or retaining possible interactions between the  $\text{NH}_2$  and OH moieties.

The source of negative signals at the  $m/z = 73$  amu mass channel has already been discussed in our previous study,<sup>41</sup> and here we briefly reiterate it for further clarification. As mentioned above, the mass spectrum<sup>41</sup> through single photon ionization of valine at 10.5 eV shows, among others, two fragment ions at  $m/z = 73$  and 30 amu. Vibrational features monitored in mass channel 73 amu arise from a loss of intensity in the mass channel, whereas those obtained by monitoring the mass channel  $m/z = 30$  amu are found to arise from a gain in intensity in the mass channel. Both of these spectra, however, show two identical features in the  $\text{NH}_2$  stretching range, which belong to conformer II of valine. This observation evidences that both fragment signals at  $m/z = 73$  and 30 amu arise from the conformer II. Fragmentation of the

radical cation intermediate of conformer II begins with hydrogen transfer from COOH to the  $\alpha$ - $\text{NH}_2$  group, followed by  $\text{C}_\alpha$ - $\text{C}_{\text{COOH}}$  bond dissociation. This pathway produces  $(\text{CH}_3)_2\text{CHCHNH}_3^+$  ( $m/z = 73$  amu). In the presence of absorbed IR radiation in the neutral molecule, the ionized valine generates a more energetic cation that can surmount the barrier to another fragmentation channel, generating  $\text{CHNH}_3^+$  ( $m/z = 30$  amu). This latter channel reduces the number of valine cations fragmenting into the  $m/z = 73$  amu channel, and the signal intensity in this fragmentation channel is thereby reduced; a negative dip spectrum is thus observed in the  $m/z = 73$  amu mass channel. Our previous study<sup>41</sup> suggests that this new channel can be associated with generation of the  $\text{CHNH}_3^+$  ion due to additional fragmentation of the  $(\text{CH}_3)_2\text{CHCHNH}_3^+$  ion.

The fragment signal at  $m/z = 72$  amu can be related to the direct  $\text{C}_\alpha$ - $\text{C}_{\text{carboxylic}}$  bond dissociation pathway for all three conformers of valine. The IR spectrum (Fig. 8) obtained by monitoring this fragment signal shows one hydrogen bonded NH stretch ( $3309\text{ cm}^{-1}$ ) and one free NH stretch ( $3409\text{ cm}^{-1}$ ); the position of each feature is clearly different from that obtained at the fragment mass channel  $m/z = 73$  amu. The IR spectrum obtained monitoring the fragment signal at  $m/z = 72$  amu is also in agreement with the calculated scaled vibrational frequencies for conformer I. In addition, each spectral feature obtained monitoring the fragment signal at  $m/z = 72$  amu is associated with a weak shoulder, the position of which is slightly blue to the more intense feature. The shoulder peaks are in good agreement with the calculated scaled vibrational frequencies of free and hydrogen bonded NH stretches for conformer III. As mentioned above with regard to the line widths of the NH stretch modes observed in Fig. 8, the isopropyl group conformations may also be a reason that the carboxyl OH transition near  $3575\text{ cm}^{-1}$  is both weak and broad for conformers I and III.

Thus, conformers I and II of both radical cationic glycine and valine dissociate through two distinctly different decomposition pathways. Conformer I undergoes direct  $\text{C}_\alpha$ - $\text{C}_{\text{carboxylic}}$  bond dissociation, whereas conformer II undergoes hydrogen transfer followed by  $\text{C}_\alpha$ - $\text{C}_{\text{carboxylic}}$  bond dissociation. Thus radical cationic reactivity of glycine and valine, which are  $\alpha$ -amino aliphatic carboxylic acids, is shown to be conformation specific. Conformer III for glycine and valine follows a direct  $\text{C}_\alpha$ - $\text{C}_{\text{carboxylic}}$  bond dissociation pathway.

## Theoretical results

Specific knowledge of the molecular ion state produced upon sudden removal of an electron from a molecule is essential in order to determine the likely fragmentation mechanisms of the nascent radical cation. Here we determine relevant molecular ion states produced by vertical ionization at 10.5 eV from comparison between the computed (at MP2/aug-cc-pVDZ)  $E_{\text{VI}}$  and the experimental ionization energy (10.5 eV), coupled with available photoelectron spectroscopy data<sup>42</sup> (Table T1 in Supporting Information). These analyses indicate that ionization of lactic acid, pyruvic acid, glycine, and valine at 10.5 eV efficiently populates only the ground doublet molecular (radical cation) ion state ( $\text{D}_0$ ).

In the one electron model (Koopmans' theorem),<sup>43</sup> removal of an electron from a neutral molecule creates a hole in the molecular electronic distribution that resides at the singly occupied molecular orbital (SOMO) of the nascent radical cation. The SOMO, therefore, represents the electronic character of the nascent molecular cation, which specifies the potential energy landscape for the cation. The hole densities for the SOMO of the three different conformers of lactic acid and pyruvic acid at the Franck–Condon point on the  $D_0$  surface, computed at the CASSCF(9,8)/6-31G(d) level of theory, are shown in Fig. 1. The two colors indicate the plus and minus phases of wavefunctions. For conformer I of lactic acid, the SOMO is entirely localized on the  $\alpha$ -hydroxy O atom ( $np_O$ ) of the molecular ion, which is notably perpendicular to the  $C_\alpha$ – $C_{\text{carboxylic}}$   $\sigma$  bond. For conformer II, the SOMO is delocalized over the nonbonding orbitals of the  $\alpha$ -hydroxy O ( $np_O$ ), carbonyl O ( $n\sigma_O$ ), and the  $C_\alpha$ – $C_{\text{carboxylic}}$   $\sigma$  bond. Furthermore, the  $np_O$  of the  $\alpha$ -hydroxyl O atom in conformer II is almost parallel to the  $C_\alpha$ – $C_{\text{carboxylic}}$  bond. For conformer III of lactic acid, on the other hand, the SOMO is entirely localized on the carbonyl O atom ( $n\sigma_O$ ). Therefore, the localization sites of the hole in the nascent, Franck–Condon, vertical radical cation of lactic acid on the  $D_0$  surface are clearly conformation specific.

For both conformers I and II of pyruvic acid, the SOMO is delocalized over the non bonding orbitals of the  $\alpha$ -carbonyl O atom, the carboxylic acid carbonyl O atom, and the  $C_\alpha$ – $C_{\text{carboxylic}}$   $\sigma$  bond with predominant contribution from the  $\alpha$ -carbonyl O atom. For conformer III, the SOMO is localized primarily on the  $\alpha$ -carbonyl O atom of the radical cation. Additionally, the  $np_O$  of the  $\alpha$ -carbonyl oxygen atom is parallel to the  $C_\alpha$ – $C_{\text{carboxylic}}$  bond for all three conformers of pyruvic acid. Therefore, contrary to the lactic acid conformers, localization site of the hole in the nascent radical cation of pyruvic acid on the  $D_0$  surface is not entirely conformer dependent.

The density for the SOMO of the different vertical ion conformers of glycine and valine on their  $D_0$  ion surface computed at the CASSCF(9,8)/6-31G(d) level of theory are shown in Fig. 6. For conformers I and III of glycine and valine, the SOMO is located on the  $\alpha$ -amine N ( $np_N$ ) of the molecular Franck–Condon ion. For glycine, the  $np_N$  in conformer I is parallel to the  $C_\alpha$ – $C_{\text{carboxylic}}$  bond and in conformer III, it is perpendicular to the  $C_\alpha$ – $C_{\text{carboxylic}}$  bond. Both conformers I and III of valine, however, have an  $np_N$  parallel to the  $C_\alpha$ – $C_{\text{carboxylic}}$  bond. For conformer II of glycine and valine, the SOMO, on the other hand, is primarily localized on the carbonyl O atom of the molecular ion. These assignments for the SOMO of  $\alpha$ -amino carboxylic acids are in good agreement with what has been recently suggested for a structurally similar alanine radical cation by Powis *et al.*<sup>44</sup> Therefore, the localization site for the hole of conformer I and II of glycine and valine in  $D_0$  state is clearly conformation specific.

Following sudden removal of an electron from a molecule, the nascent radical cation is typically not formed in its equilibrium geometry. On the femtosecond time scale, the Franck–Condon ion will evolve to the adiabatic ion while lowering its electronic energy through structural rearrangement.

The excess energy ( $E_{V1} - E_{A1}$ ) due to vertical to adiabatic evolution is stored in the vibration of the bonds of the molecular ion under isolated conditions; this vibrational energy can often cause the dissociation of the radical cation. In some cases, following vertical to adiabatic evolution of the ion, hydrogen transfer provides additional excess energy ( $E_{V1} - E_{A1} + \Delta H_{\text{reaction}}$ ) to surmount the energy barrier for molecular dissociation.<sup>41</sup> The total  $\Delta H_{\text{rxn}}$  for the rearrangement reaction can be computed using thermochemical calculations; however, such calculations alone are not sufficient for the exploration of fragmentation pathways of radical cation intermediates of bioactive carboxylic acids because a unimolecular fragmentation reaction is likely to occur through the lowest activation barrier, not necessarily for the reaction that is most exothermic. As a result, the energy barrier to the transition state to form a certain product becomes an important consideration. In general, a lower barrier for a reaction renders a unimolecular fragmentation reaction faster; moreover, a lower activation barrier channel is more likely to dominate if an equilibrium is not established prior to the reaction.

The product distributions observed through mass spectrometry following single photon VUV (10.5 eV) ionization of  $\alpha$ -substituted bioactive aliphatic carboxylic acids indicate that the initial step in the decomposition of their radical cation intermediates involves two common mechanisms: (1) a hydrogen transfer (either from the carboxylic acid group to the  $\alpha$ -substituent or *vice versa*); and (2) direct  $C_\alpha$ – $C_{\text{carboxylic}}$  bond dissociation. Therefore, we consider below the theoretical exploration of these two channels of decomposition in order to judge which of them is energetically or dynamically more favorable for a particular conformer.

The potential energy diagrams along the two reaction pathways (hydrogen transfer and COOH elimination) for different conformers of radical cationic lactic acid, pyruvic acid, glycine, and valine on the  $D_0$  surfaces, obtained at the CASSCF(9,8)/6-31G(d) level of theory, are shown in Fig. 9–12, respectively. The hydrogen transfer pathway is indicated by adding a suffix 'a,' and  $C_\alpha$ – $C_{\text{carboxylic}}$  bond dissociation pathway is referred including a suffix 'b' in the aforementioned figures.

The potential energy diagram of lactic acid on its  $D_0$  ion surface (Fig. 9) reveals that the direct  $C_\alpha$ – $C_{\text{carboxylic}}$  bond dissociation pathway is the minimum energy pathway (associated with the lowest activation barrier) for conformers II and III. Therefore, these two conformers will lead to a predominately kinetically controlled product at low temperature through this dissociation channel. The  $C_\alpha$ – $C_{\text{carboxylic}}$  bond dissociation pathway possesses, however, different exothermicities for these two conformers (–17 kcal/mol for conformer II and –8 kcal/mol for conformer III). The hydrogen transfer pathway (from  $\alpha$ -OH to COOH), on the other hand, is computed to be the minimum energy pathway for conformer I of lactic acid.

At the CASSCF level, a ( $D_1/D_0$ )<sub>CI</sub> conical intersection of lactic acid is localized in the hydrogen transfer reaction coordinate, as illustrated in Fig. 13. An adiabatic energy gap between  $D_1$  and  $D_0$  surfaces in the conical intersection is calculated to be  $400 \text{ cm}^{-1}$ , indicating a strong nonadiabatic coupling between  $D_1$  and  $D_0$  surfaces. As mentioned previously, ground electronic surface topology is found to be affected by

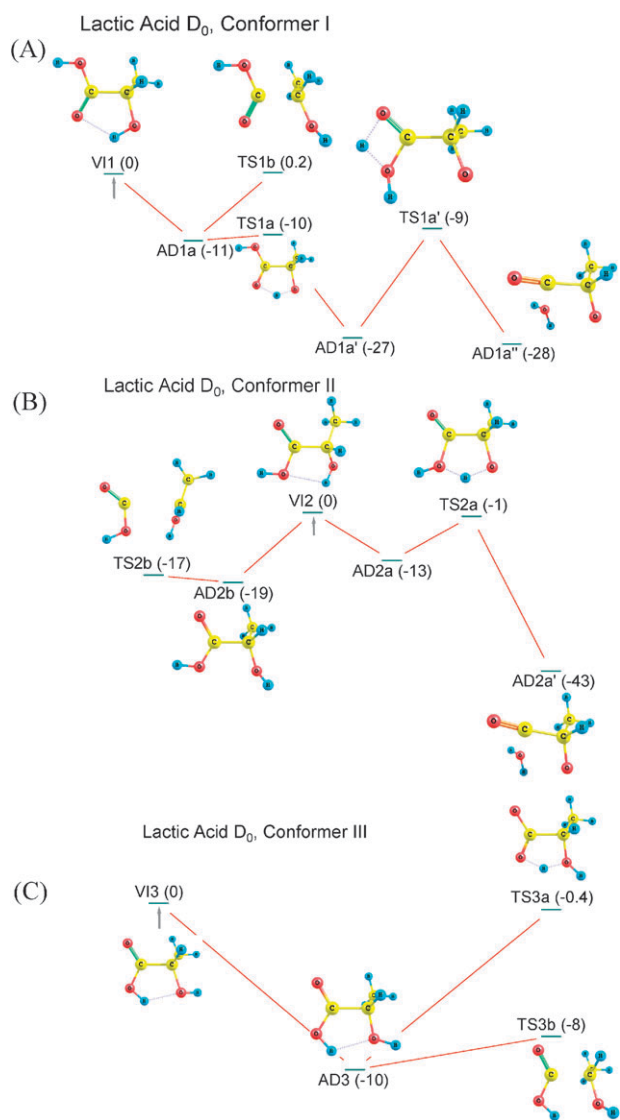


**Fig. 9** Potential energy diagram for lactic acid on its  $D_0$  ion surface calculated at the CASSCF(9,8)/6-31G(d) level of theory. Two decomposition pathways are shown: (a) hydrogen transfer, and (b) direct  $C_\alpha$ - $C_{\text{carboxylic}}$  bond dissociation. Relative energies are in kcal/mol. Vertical arrows show the accessed Franck–Condon point for the ion.

the proximity of the upper excited electronic surface near the conical intersection.<sup>45</sup> Clearly, these results provide further justification for utilizing a multiconfigurational method such as CASSCF in order to fully explore such effects.

Furthermore, a hydrogen transfer reaction is considered to be the minimum energy pathway for conformer I of lactic acid, regardless of which doublet electronic state is accessed through the 10.5 eV radiation. The conical intersection located at the reaction coordinate ensures that similar chemistry will occur on both the  $D_0$  and  $D_1$  surfaces.

The potential energy diagram of pyruvic acid on its  $D_0$  ion surface (Fig. 10) indicates that the  $C_\alpha$ - $C_{\text{carboxylic}}$  bond dissociation is the minimum energy pathway for all three conformers of pyruvic acid. A zero activation barrier exists in this reaction coordinate for all three conformers. The computed activation barrier from the Franck–Condon point on the  $D_0$  surface of

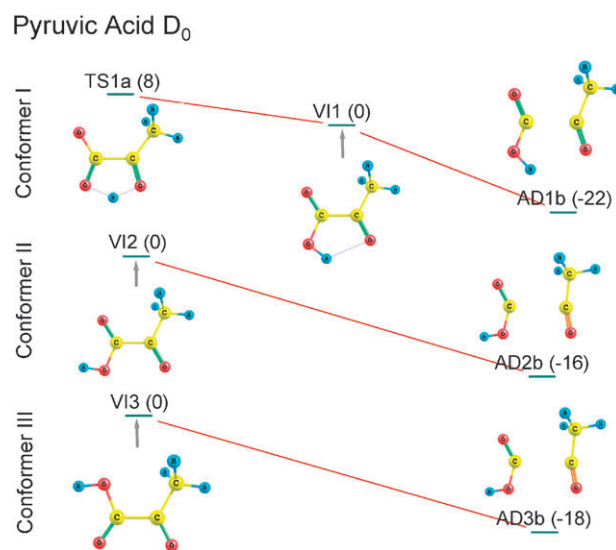


**Fig. 10** Potential energy diagram for pyruvic acid on its  $D_0$  ion surface calculated at the CASSCF(9,8)/6-31G(d) level of theory. Two decomposition pathways are shown: (a) hydrogen transfer, and (b) direct  $C_\alpha$ - $C_{\text{carboxylic}}$  bond dissociation. Relative energies are in kcal/mol. Vertical arrows show the accessed Franck–Condon point for the ion.

pyruvic acid shows hydrogen transfer from COOH to the  $\alpha$ -keto substituent, on the other hand, as a highly endothermic process (by 8 kcal/mol). Therefore, hydrogen transfer for this cation should not (and does not) occur for conformer I.

The potential energy diagram for glycine on its  $D_0$  surface (Fig. 11) shows that a  $C_\alpha$ - $C_{\text{carboxylic}}$  bond dissociation is the minimum energy pathway for conformers I and III. This reaction coordinate possesses a zero activation energy for conformer I and an activation energy of 16 kcal/mol for conformer III. The hydrogen transfer pathway, however, is the minimum energy pathway for conformer II of glycine. A zero activation energy barrier exists in the  $C_\alpha$ - $C_{\text{carboxylic}}$  bond dissociation pathway for conformers I and III of valine (Fig. 12). The hydrogen transfer pathway for valine is calculated to be the minimum energy pathway for conformer II.

To obtain further information on the ground doublet ion surface topology of conformer II of glycine, we investigate the influence of  $(D_1/D_0)_{\text{CI}}$  conical intersection on the ground surface. The CASSCF calculations reveal that the upper  $D_1$  electronic surface for the conformer II is highly nonadiabatically coupled with  $D_0$  surface along the hydrogen transfer reaction coordinate. A  $(D_1/D_0)_{\text{CI}}$  conical intersection is localized in the hydrogen transfer reaction coordinate of conformer II, which is illustrated in Fig. 14. The adiabatic energy difference between the  $D_0$  and  $D_1$  surfaces near the  $(D_1/D_0)_{\text{CI}}$  conical intersection is calculated to be  $500\text{ cm}^{-1}$ , which suggests strong nonadiabatic coupling between the  $D_1$  and  $D_0$  surfaces. Again, the multiconfigurational approach of CASSCF is justified.

Overall the theoretical results show that initial structures of the bioactive carboxylic acids have significant influence on their subsequent reactivity following ionization. Intramolecular hydrogen bonding can alter the local charge distribution in

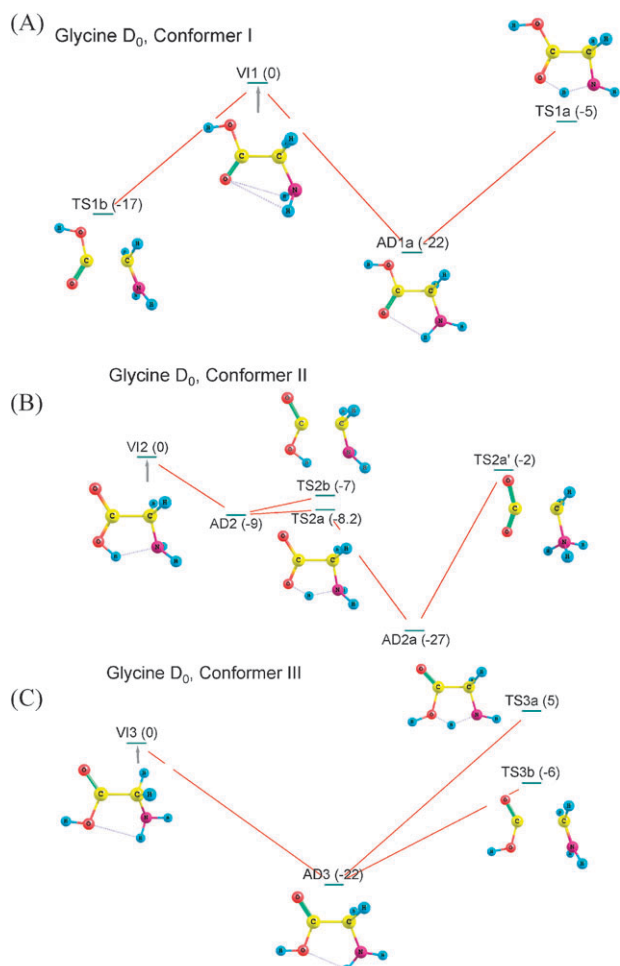


**Fig. 11** Potential energy diagram for glycine on its  $D_0$  ion surface calculated at the CASSCF(9,8)/6-31G(d) level of theory. Two decomposition pathways are shown: (a) hydrogen transfer, and (b) direct  $C_\alpha$ - $C_{\text{carboxylic}}$  bond dissociation. Relative energies are in kcal/mol. Vertical arrows show the accessed Franck–Condon point for the ion.

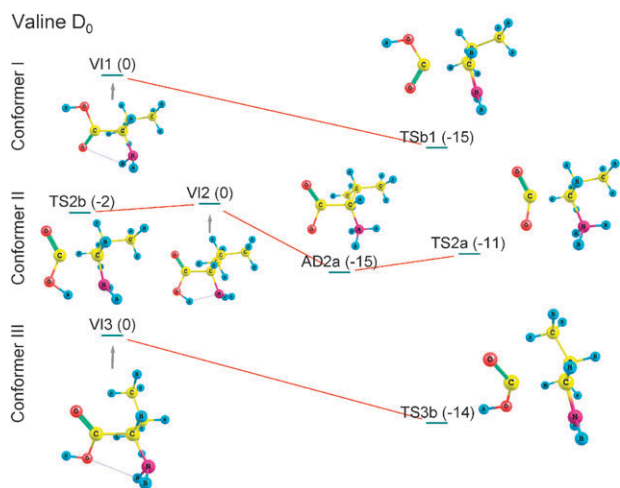


**Fig. 12** Potential energy diagram for valine on its  $D_0$  ion surface calculated at the CASSCF(9,8)/6-31G(d) level of theory. Two decomposition pathways are shown: (a) hydrogen transfer, and (b) direct  $C_\alpha$ - $C_{\text{carboxylic}}$  bond dissociation. Relative energies are in kcal/mol. Vertical arrows show the accessed Franck–Condon point for the ion.

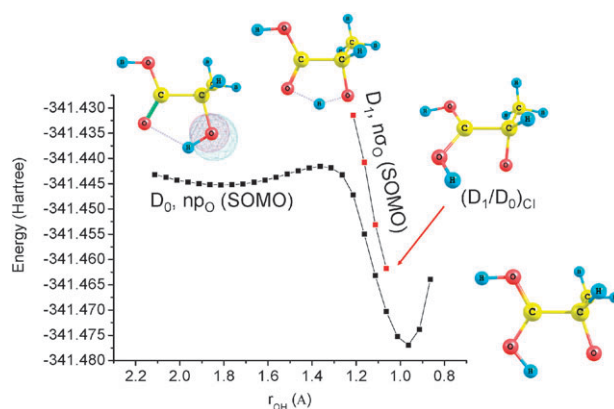


**Fig. 13** Hydrogen transfer pathways for conformer I with location of the  $(D_1/D_0)_{CI}$  conical intersection computed at CASSCF(9,8)/6-31G(d) level of theory.

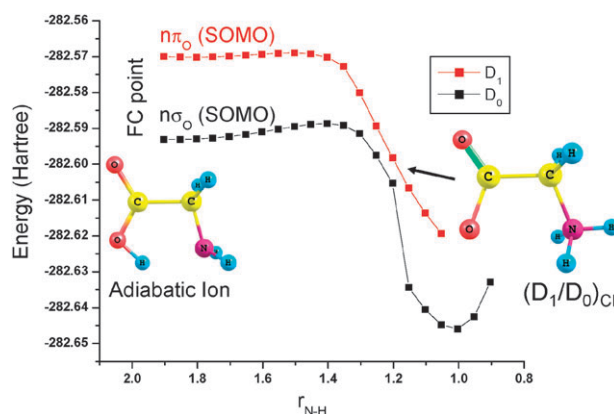


**Fig. 14** Hydrogen transfer pathway for conformer II of glycine with localization of  $(D_1/D_0)_{CI}$ . FC = Franck–Condon.

these radical cation intermediates. Moreover, a relationship between charge, structure, and reactivity emerges from this study. If the charge is localized on the carboxylic acid group, a hydrogen transfer is favored from COOH to the  $\alpha$ -substituent. If the charge is localized on the  $\alpha$ -substituent and the SOMO is parallel to the  $C_\alpha$ - $C_{\text{carboxylic}}$  bond, a charge transfer occurs to the  $C_\alpha$ - $C_{\text{carboxylic}}$  bond, facilitating a direct  $C_\alpha$ - $C_{\text{carboxylic}}$  bond dissociation without any activation energy barrier. These theoretical findings fully corroborate the experimental observations.

## Discussion

A number of observations are crucial for understanding the conformation specific reactivity of radical cation intermediates of  $\alpha$ -substituted bioactive carboxylic acids. Undoubtedly, if the excess energy, obtained through the vertical to adiabatic evolution of the molecular ion, is enough to surmount the activation energy needed to initiate a decomposition reaction, fragmentation of radical cation intermediates takes place. This excess energy may also result in the interconversion between different cation conformations. The interconversion energy for lactic acid, glycine, and valine on their ground cation

surface is computed to be within the range of 2–6 kcal/mol, which is much smaller than the available excess energy (ranging from 10 to 20 kcal/mol) stored in the molecular vibrations following vertical ionization. Therefore, identical products could possibly be generated from different conformers through interconversion following ionization, which can diminish conformation specific behavior. This consideration, however, can be ruled out: the significant difference in IR spectra (Fig. 3 and 8 for lactic acid and valine, respectively) recorded by monitoring the fragment signals does not suggest such an interconversion. The IR spectra recorded at different fragment signals are distinctly different for lactic acid and valine,<sup>41</sup> and they do not appear to be the superposition of two or more components. This suggests that VUV photoionization does not induce interconversion of the radical cation intermediates of lactic acid and valine. Instead, different conformers move along different reaction pathways following ionization. Thus, the vertical to adiabatic evolution and subsequent fragmentation are faster than the conformational interconversion. The fragmentation dynamics of the radical cation intermediates of these two bioactive carboxylic acids studied in the present work are, therefore, predicted to be ultrafast so that each molecule retains the memory of its original conformation.

Both the mechanism for radical cation formation (*e.g.*, electron impact or single photon ionization) and the radical cation's position on the ion potential energy surface (*e.g.*, Franck–Condon, adiabatic, *etc.*) can be essential factors for the radical cation relaxation and/or unimolecular reaction. Details of the PES barriers for conformer interconversion and fragmentation reactions control the initial radical cation behavior: which pathway will dominate depends entirely on which part of the PES is accessed by the molecule following photoionization. This fact is directly evidenced by the present IR-VUV spectroscopic study of lactic acid and by our previous valine study.<sup>41</sup> The vibrational features observed in the pyruvic acid parent mass channel arise from contributions from different conformers present in the molecular beam. No vibrational features are observed in the fragment ion mass channel.

The theoretical results demonstrate that the direct  $C_{\alpha}$ – $C_{\text{carboxylic}}$  bond dissociation channel requires a specific conformational orientation such that the SOMO (usually a nonbonding p-orbital) on the  $\alpha$ -substituent stays parallel to the  $C_{\alpha}$ – $C_{\text{carboxylic}}$   $\sigma$  bond (see the following structures: TS1b, AD2b, and TS3b of lactic acid in Fig. 9; TS1b, TS3b of glycine in Fig. 11; and TS1b, TS3b of valine in Fig. 12). This suitable geometrical orientation facilitates hole migration from  $2p_{\text{O}}$  (SOMO) to the  $C_{\alpha}$ – $C_{\text{carboxylic}}$   $\sigma$  bond. This charge migration (or hole transfer) initiates direct  $C_{\alpha}$ – $C_{\text{carboxylic}}$  bond dissociation because the bond that breaks is the one to which the hole is finally localized in the radical cation. Conformers that have the SOMO localized on the  $\alpha$ -substituent and parallel to the  $C_{\alpha}$ – $C_{\text{carboxylic}}$  bond at the Franck–Condon point on the cationic surface, can undergo ultrafast (expected to be on attosecond time scale)<sup>46,47</sup> charge migration from the  $\alpha$ -substituent to the  $C_{\alpha}$ – $C_{\text{carboxylic}}$  bond and can thereby generate direct COOH elimination products. Such conformers include conformer II of lactic acid, all three

conformers of pyruvic acid, conformer I of glycine, and conformers I and III of valine. All these conformers require no activation energy for the  $C_{\alpha}$ – $C_{\text{carboxylic}}$  bond dissociation reaction pathway from the Franck–Condon point on the  $D_0$  surface (Fig. 9–12).

Conformers for which the SOMO is localized on the  $\alpha$ -substituent and for which a structural rearrangement is required to make the SOMO parallel to the  $C_{\alpha}$ – $C_{\text{carboxylic}}$  bond possess a finite activation barrier for the  $C_{\alpha}$ – $C_{\text{carboxylic}}$  bond dissociation. This mechanism is exemplified by conformer I of lactic acid and conformer III of glycine. Conformers for which the SOMO is localized on the carboxylic acid group undergo hydrogen transfer from the carboxylic acid group to the  $\alpha$ -substituent. This mechanism occurs for conformer III of lactic acid and conformer II of glycine and valine.

Thus, conformation specific reactivity of radical cation intermediates is solely directed by two specific properties of the molecular ion: 1. the specific localization of the charge; and 2. the initial intramolecular hydrogen bonding structure. The hydrogen bonding structure of these species can favor or hinder charge migration and hydrogen transfer. This conclusion is consistent with the idea of a ‘charge directed reactivity’ of peptides observed by Weinkauff *et al.*<sup>23a</sup> Their study finds that fragmentation products of peptides, generated by vertical ionization, depend upon specific peptide sequences that can assist or hinder hole migration. Weinkauff *et al.*<sup>23b</sup> later modeled charge propagation within a peptide as arising from a steric requirement for bond alignment along the peptide chain to facilitate hole migration. We also find similar steric requirements for charge transfer to occur from the SOMO on the  $\alpha$ -substituent to the  $C_{\alpha}$ – $C_{\text{carboxylic}}$  bond for  $\alpha$ -substituted carboxylic acids. Thus a ‘through bond’ mechanism<sup>45</sup> is supported for charge migration. Knowledge of the relative timescales (barriers) of charge transfer, hydrogen transfer, and structural change is essential in order to obtain further detailed insights on the interplay of these three processes for the reactivity of radical cation intermediates of  $\alpha$ -substituted bioactive carboxylic acids.

Radical cationic pyruvic acid shows a special stability with respect to lactic acid, glycine, and valine. A qualitative comparison of mass spectral intensities between the parent ion and fragment ion signals for pyruvic acid indicates that less than 45% of pyruvic acid parent ions dissociate following VUV ionization at 10.5 eV. Our present computational results show that single photon ionization of pyruvic acid at 10.5 eV provides sufficient excess vibrational energy ( $E_{\text{VI}} - E_{\text{AI}}$ ) to surmount the energy barrier for dissociation on the ground ion surface. In fact, C–C bond dissociation is predicted to be barrierless from the Franck–Condon point on the adiabatic ion surface. Therefore, complete fragmentation can be expected for this molecular ion; however, our experimental results do not support such a conclusion. A recent theoretical study by Raczyńska *et al.*<sup>12</sup> has shown that  $\pi$ -delocalization of the positive charge following enolization of the  $\alpha$ -keto form provides extra stability to the radical cation intermediate of pyruvic acid. A similar stabilization effect does not exist for the lactic acid radical cation. Difference in the ionization energy for the two molecules [ $E_{\text{VI}}(\text{pyruvic}) - E_{\text{VI}}(\text{lactic})$ , 0.023 eV] (Table T1 in Supporting Information) has little

effect on the differences in their fragmentation pathways, as the excess photon energy ( $10.5 \text{ eV} - E_{\text{VI}}$ ) following ionization is converted into photoelectron kinetic energy due to energy conservation ( $E_{\text{K}} = E_{h\nu} - E_{\text{VI}}$ ): fragmentation is governed by the excess vibrational energy [ $E_{\text{VI}} - E_{\text{AI}}$ ,  $0.81 \text{ eV}$  (calculated from Fig. 10)] of the cation and the shape of potential energy surface leading to the adiabatic ion state.

Thermochemical calculations (Reaction R1 in Supporting Information) for lactic acid predict that the two fragment ions at  $m/z = 30$  and  $44$  amu can be generated on the cation's ground PESs of lactic acid, following  $10.5 \text{ eV}$  vertical photoionization. Photoionization of lactic acid at  $10.5 \text{ eV}$  does not evidence a fragment at mass channel  $m/z = 45$  amu corresponding to direct  $\text{C}_{\alpha}\text{-C}_{\text{carboxylic}}$  bond dissociation, as this fragment can further dissociate to the  $m/z = 30$  amu ion. Electron impact (EI) ionization,<sup>48</sup> which generates the  $m/z = 45$  amu ion, is not directly relevant to the photoionization results because EI ionization does not necessarily place the created ion at the Franck–Condon point or even on the same PES as does photoionization.<sup>49</sup>

## Conclusions

In this work, we illustrate the conformation specific and charge directed reactivity of the radical cation intermediates of lactic acid, pyruvic acid, glycine, and valine. The conformation specificity and charge directed reactivity suggested for these systems can be generalized for radical cation intermediate behavior for all bioactive carboxylic acids. Lactic acid, glycine, and valine, when ionized to the lowest vertical ionization region, undergo complete and conformation specific fragmentation. Conformational analysis for each molecule is carried out through IR spectroscopy complemented by theoretical results.

Conformers of these molecules, for which the  $\alpha$ -substituent donates a hydrogen bond to the carboxylic acid group, favor either  $\text{C}_{\alpha}\text{-C}_{\text{carboxylic}}$  bond dissociation or hydrogen transfer from the  $\alpha$ -substituent to the carboxylic acid group. The hydrogen transfer, however, depends on the activation barrier and the relative orientation of the singly occupied molecular orbital with respect to the  $\text{C}_{\alpha}\text{-C}_{\text{carboxylic}}$  bond. Conformers for which the  $\alpha$ -substituent of these molecules accepts a hydrogen bond from the carboxylic acid OH facilitate hydrogen transfer from the carboxylic acid OH to the  $\alpha$ -substituent. Pyruvic acid, on the other hand, does not undergo complete dissociation following ionization, resulting in a stable radical cation. We have identified two different conformers of pyruvic acid, both of which undergo, to some extent,  $\text{C}_{\alpha}\text{-C}_{\text{carboxylic}}$  dissociation; however, the reaction pathways associated with  $\text{C}_{\alpha}\text{-C}_{\text{carboxylic}}$  dissociation for the two conformers have different exothermicities. Thus, the reactivity and stability of radical cationic bioactive carboxylic acids is dependent on the properties of their original conformations.

*Ab initio* calculations show that the electronic hole (positive charge) in the nascent radical cationic lactic acid, glycine, and valine is primarily localized on the hydroxyl O or amine N atom if the  $\alpha$ -substituent donates a hydrogen bond to the carboxylic acid group (conformers I and II of lactic acid,

and I and II of glycine and valine). This structure favors either  $\text{C}_{\alpha}\text{-C}_{\text{carboxylic}}$  bond dissociation or hydrogen transfer from the  $\alpha$ -substituent to the carboxylic acid group. The actual mechanism, however, depends on the relative orientation of the SOMO with respect to the  $\text{C}_{\alpha}\text{-C}_{\text{carboxylic}}$   $\sigma$ -bond and the activation barrier associated with the reaction coordinate. If the  $\alpha$ -substituent accepts a hydrogen bond from the carboxylic acid OH group (conformer III of lactic acid and II of glycine and valine), a stabilization effect due to hydrogen bonding lowers the energy of the lone pair orbitals of the  $\alpha$ -substituent. In this case, the hole is localized on the carboxylic acid group, and this structure facilitates hydrogen transfer from carboxylic acid OH to the  $\alpha$ -substituent. Thus, different structural orientations of the molecule give rise to different fragmentation patterns in  $\alpha$ -hydroxy and  $\alpha$ -amino aliphatic bioactive carboxylic acids: the reactivity of these systems is primarily governed by the local charge distribution.

The pyruvic acid radical cation, generated near its lowest vertical ionization region, does not completely undergo fragmentation. Two different conformers (I and II) of pyruvic acid are identified by recording IR spectra monitoring the parent ion signal. Both conformers undergo, to some extent, the  $\text{C}_{\alpha}\text{-C}_{\text{carboxylic}}$  bond dissociation; however, theoretical calculations infer that different exothermicities of the reaction associated with the two conformers may provide different energy distributions for the products ( $\text{COOH}$  and  $\text{H}_3\text{CCO}^+$ ).

Comparison of the IR spectra with the calculated harmonic frequencies of different conformers has enabled the identification of conformers with particular fragment channels. The IR spectra obtained at fragment and parent mass channels are in good agreement with the scaled (0.96) harmonic calculated harmonic frequencies of different conformers of lactic acid, valine, glycine, and pyruvic acid. Therefore, although signal to noise ratio in these spectra is not optimal for the features associated with hydrogen bonded or free OH and  $\text{NH}_2$  groups, comparison of experiment and theory provides clear information about the conformers.

In order to study the role of the local ion environment on conformation specific reactivity and stability of isolated biomolecules further, we have started experiments on simple  $\alpha$ -substituted amides, and  $\beta$ -hydroxy/thiol amino acids. All these hitherto unexplored systems are in principle open to IR-VUV photoionization spectroscopic study. Other experiments that would be helpful in further exploring conformation specificity for the reactivity of radical cation intermediates include velocity map imaging experiments to measure different components of translational energy distribution following  $\text{C}_{\alpha}\text{-C}_{\text{carboxylic}}$  bond dissociation from different conformers, and photoelectron spectroscopy to determine the molecular ion states. Also, theoretical exploration of the relative time scales of charge transfer, hydrogen transfer, and structural rearrangement for a particular conformer of bioactive carboxylic acids would be advantageous.

## Acknowledgements

Parts of these studies are supported by grants from the US ARO and NSF.

## References

- 1 (a) B. S. Berlett and E. R. Stadtman, *J. Biol. Chem.*, 1997, **272**, 20313; (b) E. R. Stadtman, *Annu. Rev. Biochem.*, 1993, **62**, 797; (c) M. J. Davis and R. J. W. Truscott, *J. Photochem. Photobiol., B*, 2001, **63**, 114; (d) R. V. Bensasson, E. J. Land and T. G. Truscott, *Excited States and Free Radicals in Biology and Medicine*, Oxford University Press, New York, 1983; (e) J. Stubbe and W. A. van der Donk, *Chem. Rev.*, 1998, **98**, 705.
- 2 (a) S. Varadarajan, S. Yatin, J. Kanshi and F. Jahanshahi, *Brain Res. Bull.*, 1999, **50**, 133; (b) C. Schoneich, D. Pogocki, G. L. Hug and K. Bobrowski, *J. Am. Chem. Soc.*, 2003, **125**, 13700; (c) H. Yashiro, R. C. White, A. V. Yurkovskaya and M. D. E. Forbes, *J. Phys. Chem. A*, 2005, **109**, 5855.
- 3 M. Kantorow, J. R. Hawse, T. L. Cowell, S. Benhamed, G. O. Pizarro, V. N. Reddy and J. F. Heijtmancik, *Proc. Natl. Acad. Sci. U. S. A.*, 2004, **101**, 9654.
- 4 (a) J. S. Splitter and F. Turecek, *Application of Mass Spectrometry to Organic Stereo Chemistry*, Wiley-VCH, Inc, New York, 1994; (b) C. K. Barlow, D. Moran, L. Random, W. D. McFadyen and R. A. J. O'Hair, *J. Phys. Chem. A*, 2006, **110**, 8304.
- 5 (a) V. Chis, M. Brustolon, C. Morari, O. Cozar and L. David, *J. Mol. Struct.*, 1999, **482**, 283; (b) M. Brustolon, V. Chis, A. L. Maniero and L. C. Brunel, *J. Phys. Chem. A*, 1997, **101**, 4887.
- 6 A. Sanderud and E. Sagstuen, *J. Phys. Chem. B*, 1998, **102**, 9353.
- 7 C. L. Hawkins and M. J. Davis, *J. Chem. Soc., Perkin Trans. 2*, 1998, 2617.
- 8 G. L. Hug and R. W. Fessenden, *J. Phys. Chem. A*, 2000, **104**, 7021.
- 9 M. Bonifacic, I. Stefanic, G. L. Gug, D. A. Armstrong and K.-D. Asmus, *J. Am. Chem. Soc.*, 1998, **120**, 9930.
- 10 D. A. Armstrong, A. Rauk and D. Yu, *J. Chem. Soc., Perkin Trans. 2*, 1995, 553.
- 11 (a) K. N. Sutherland, P. C. Mineau and G. Orlova, *J. Phys. Chem. A*, 2007, **111**, 7906; (b) S. Simon, M. Sodupe and J. Bertran, *J. Phys. Chem. A*, 2002, **106**, 5697.
- 12 E. D. Raczynska, M. Hallmann and K. Duczmal, *J. Iran. Chem. Res.*, 2008, **1**, 57.
- 13 A. Rauk, D. Yu and D. A. Armstrong, *J. Am. Chem. Soc.*, 1997, **119**, 208.
- 14 D. Yu, A. Rauk and D. A. Armstrong, *J. Am. Chem. Soc.*, 1995, **117**, 1789.
- 15 V. Barone, C. Adamo, A. Grand, F. Jolibois, Y. Brunel and R. Subra, *J. Am. Chem. Soc.*, 1995, **117**, 12618.
- 16 V. Barone, C. Adamo, A. Grand and R. Subra, *Chem. Phys. Lett.*, 1995, **242**, 351.
- 17 N. Rega, M. Cossi and V. Barone, *J. Am. Chem. Soc.*, 1997, **119**, 12962.
- 18 N. Rega, M. Cossi and V. Barone, *J. Am. Chem. Soc.*, 1998, **120**, 5723.
- 19 F. Ban, J. W. Gauld and R. J. Boyd, *J. Phys. Chem. A*, 2000, **104**, 5080.
- 20 F. Ban, S. D. Wetmore and R. J. Boyd, *J. Phys. Chem. A*, 1999, **103**, 4303.
- 21 F. Himo and L. A. Ericksson, *J. Chem. Soc., Perkin Trans. 2*, 1998, 305.
- 22 L. Rodriguez-Santiago, M. Sodupe, A. Oliva and J. Bertran, *J. Phys. Chem. A*, 2000, **104**, 1256.
- 23 (a) R. Weinkauff, P. Schanen, D. Yang, S. Soukara and E. W. Schlag, *J. Phys. Chem.*, 1995, **99**, 11255; (b) R. Weinkauff, P. Schanen, A. Metsala, E. W. Schlag, M. Burtle and H. Kessler, *J. Phys. Chem.*, 1996, **100**, 18567; (c) I. K. Chu, C. F. Rodriguez, T. Lau, A. C. Hopkinson and K. W. M. Siu, *J. Phys. Chem. B*, 2000, **104**, 3393; (d) C. K. Barlow, S. Wee, W. D. McFadyen and R. A. J. O'Hair, *Dalton Trans.*, 2004, (20), 3199; (e) F. Turecek, F. H. Carpenter, M. J. Polce and C. Wesdemiotis, *J. Am. Chem. Soc.*, 1999, **121**, 7955; (f) A. C. Hopkinson and K. W. M. Siu, In *Peptide Radical Cations in: Principles of Mass Spectrometry Applied to Biomolecules*, ed. J. Laskin and C. Lifshitz, John Wiley and Sons, NJ, 2006, pp. 301–335.
- 24 (a) F. Remacle and R. D. Levine, *Proc. Natl. Acad. Sci. U. S. A.*, 2006, **103**, 6793; (b) F. Remacle and R. D. Levine, *Z. Phys. Chem.*, 2007, **221**, 647.
- 25 A. I. Kuleff and L. S. Cederbaum, *Chem. Phys.*, 2007, **338**, 320.
- 26 D. Shemesh and R. B. Gerber, *J. Chem. Phys.*, 2005, **122**, 241104.
- 27 (a) K.-W. Choi, D.-S. Ahn, J.-H. Lee and S. K. Kim, *Chem. Commun.*, 2007, 1041; (b) L. Zhang, Y. Pan, H. Guo, T. Zhang, L. Sheng and F. Qi, *J. Phys. Chem. A*, 2009, **113**, 5838.
- 28 (a) Y. J. Hu, H. B. Fu and E. R. Bernstein, *J. Chem. Phys.*, 2006, **125**, 184308; (b) Y. J. Hu, H. B. Fu and E. R. Bernstein, *J. Chem. Phys.*, 2006, **125**, 184309; (c) Y. J. Hu, H. B. Fu and E. R. Bernstein, *J. Chem. Phys.*, 2006, **125**, 154306; (d) H. B. Fu, Y. J. Hu and E. R. Bernstein, *J. Chem. Phys.*, 2006, **124**, 024302; (e) Y. J. Hu, H. B. Fu and E. R. Bernstein, *J. Chem. Phys.*, 2006, **125**, 154305; (f) J.-W. Shin and E. R. Bernstein, *J. Chem. Phys.*, 2009, **130**, 214306.
- 29 (a) M. Garavelli, *Theor. Chem. Acc.*, 2006, **116**, 87; (b) B. R. Smith, M. J. Bearpark, M. A. Robb, F. Bernardi and M. Olivucci, *Chem. Phys. Lett.*, 1995, **242**, 27; (c) D. R. Yarkony, *J. Phys. Chem. A*, 2001, **105**, 6277.
- 30 (a) A. Bhattacharya, Y. Q. Guo and E. R. Bernstein, *J. Phys. Chem. A*, 2009, **113**, 811; (b) J. Soto, J. F. Arenas, J. C. Otero and D. Pelaez, *J. Phys. Chem. A*, 2006, **110**, 8221.
- 31 (a) L. Blancafort, *J. Am. Chem. Soc.*, 2006, **128**, 210; (b) E. Muchova, P. Slvicek, A. L. Sobolewski and P. Hobza, *J. Phys. Chem. A*, 2007, **111**, 5259.
- 32 M. J. Frisch, G. W. Trucks, H. B. Schlegel, G. E. Scuseria, M. A. Robb, J. R. Cheeseman, J. A. Montgomery, Jr., T. Vreven, K. N. Kudin, J. C. Burant, J. M. Millam, S. S. Iyengar, J. Tomasi, V. Barone, B. Mennucci, M. Cossi, G. Scalmani, N. Rega, G. A. Petersson, H. Nakatsuji, M. Hada, M. Ehara, K. Toyota, R. Fukuda, J. Hasegawa, M. Ishida, T. Nakajima, Y. Honda, O. Kitao, H. Nakai, M. Klene, X. Li, J. E. Knox, H. P. Hratchian, J. B. Cross, V. Bakken, C. Adamo, J. Jaramillo, R. Gomperts, R. E. Stratmann, O. Yazyev, A. J. Austin, R. Cammi, C. Pomelli, J. W. Ochterski, P. Y. Ayala, K. Morokuma, G. A. Voth, P. Salvador, J. J. Dannenberg, V. G. Zakrzewski, S. Dapprich, A. D. Daniels, M. C. Strain, O. Farkas, D. K. Malick, A. D. Rabuck, K. Raghavachari, J. B. Foresman, J. V. Ortiz, Q. Cui, A. G. Baboul, S. Clifford, J. Cioslowski, B. B. Stefanov, G. Liu, A. Liashenko, P. Piskorz, I. Komaromi, R. L. Martin, D. J. Fox, T. Keith, M. A. Al-Laham, C. Y. Peng, A. Nanayakkara, M. Challacombe, P. M. W. Gill, B. Johnson, W. Chen, M. W. Wong, C. Gonzalez and J. A. Pople, *GAUSSIAN 03, Revision C.02*, Gaussian, Inc, Wallingford, CT, 2004.
- 33 H.-J. Werner and P. J. Knowles, *MOLPRO (Version 2000.1)*, University of Sussex, UK, 1999.
- 34 M. Pecul, A. Rizzo and J. Leszczynski, *J. Phys. Chem. A*, 2002, **106**, 11008.
- 35 B. van Eijck, *J. Mol. Spectrosc.*, 1983, **101**, 113.
- 36 A. Borba, A. Gomez-Zavaglia, L. Lapinski and R. Fausto, *Phys. Chem. Chem. Phys.*, 2004, **6**, 2101.
- 37 G. C. Pimentel and A. L. McClellan, *The Hydrogen Bond*, Freeman, San Francisco, 1960.
- 38 (a) C. Berthomieu and C. Sandorfy, *J. Mol. Spectrosc.*, 1965, **15**, 15; (b) G. Durocher and C. Sandorfy, *J. Mol. Spectrosc.*, 1965, **15**, 22; (c) A. Foldes and C. Sandorfy, *J. Mol. Spectrosc.*, 1966, **20**, 262; (d) E. T. J. Nibbering and T. Elsaesser, *Chem. Rev.*, 2004, **104**, 1887; (e) T. Elsaesser, N. Huse, J. Dreyer, J. R. Dwyer, K. Heyne and E. T. J. Nibbering, *Chem. Phys.*, 2007, **341**, 175; (f) V. Kozich, J. Dreyer, S. Ashihara, W. Werncke and T. Elsaesser, *J. Chem. Phys.*, 2006, **125**, 074504.
- 39 P. Tarakeswar and S. Manogaran, *J. Mol. Struct.*, 1998, **430**, 51.
- 40 K. L. Plath, K. Takahashi, R. T. Skodje and V. Vaida, *J. Phys. Chem. A*, 2009, **113**, 7294.
- 41 Y. Hu and E. R. Bernstein, *J. Chem. Phys.*, 2008, **128**, 164311.
- 42 (a) T. P. Debies and J. W. Rabalais, *J. Electron Spectrosc. Relat. Phenom.*, 1974, **3**, 315; (b) S. P. McGlynn and J. L. Meeks, *J. Electron Spectrosc. Relat. Phenom.*, 1975, **6**, 269.
- 43 G. C. Schatz and M. A. Ratner, *Quantum Mechanics in Chemistry*, Prentice-Hall, Englewood Cliffs, New Jersey, 1993.
- 44 I. Powis, E. E. Rennie, U. Hergenhaln, O. Kugeler and R. Bussy-Socrate, *J. Phys. Chem. A*, 2003, **107**, 25.

- 
- 45 R. A. Marcus and N. Sutin, *Biochim. Biophys. Acta*, 1985, **811**, 265.
- 46 N. Y. Dodonova, *J. Photochem. Photobiol., B*, 1993, **18**, 111.
- 47 G. D. Cody, N. Z. Boctor, T. R. Filley, R. M. Hazen, J. H. Scott, A. Sharma and H. S. Yoder, Jr., *Science*, 2000, **289**, 1337.
- 48 [http://webbook.nist.gov/cgi/cbook.cgi?ID = C50215&Units = SI&Mask = 200#Mass-Spec](http://webbook.nist.gov/cgi/cbook.cgi?ID=C50215&Units=SI&Mask=200#Mass-Spec).
- 49 (a) D. L. Hildenbrand, *Int. J. Mass Spectrom.*, 2000, **197**, 237; (b) M. Stano, S. Matejčík, J. D. Skalný and T. D. Märk, *J. Phys. B: At., Mol. Opt. Phys.*, 2003, **36**, 261; (c) E. Vašeková, M. Stano, Š. Matejček, J. D. Skalný, P. Mach, J. Urban and T. D. Märk, *Int. J. Mass Spectrom.*, 2004, **235**, 155.